International Journal of
Drug Discovery and Pharmacology (IJDDP)

Scilight

Article

Neuroprotective Effects of Active Component Combination from Shengmai San on Cerebral Ischemia Injury

Ling Li [1], Zhuo Yang [1], Ze-Kun Chen [1,2], Tian-Tian Wei [1], Peng-Fei Tu [1], Ying Zhou [3], Bo-Wen Pan [3], and Ke-Wu Zeng [1,2,*]

[1] State Key Laboratory of Natural and Biomimetic Drugs, School of Pharmaceutical Sciences, Peking University, Beijing, 100191, China
[2] Department of Integration of Chinese and Western Medicine, School of Basic Medical Sciences, Peking University, Beijing 100191, China
[3] College of Pharmacy, Guizhou University of Traditional Chinese Medicine, Guiyang 550025, China
* Correspondence: ZKW@bjmu.edu.cn
Received: 26 October 2025; Revised: 16 December 2025; Accepted: 17 December 2025; Published: 12 February 2026

Abstract: Background: Shengmai San (SMS), a classical traditional Chinese medicine (TCM) formulation, has been clinically used for centuries in the treatment of ischemic stroke (IS). However, the complexity of SMS leads to ambiguous bioactive components and poorly understood mechanisms of action. Therefore, the development of optimized active component combinations from SMS represents a promising strategy for novel therapeutic agents against IS. Methods: In this study, we developed an active component combination (ACCS) from SMS and evaluated the neuroprotective effect of ACCS in a rat middle cerebral artery occlusion (MCAO) model. An integrated multi-omics approach, combining 16S rRNA gut microbiota sequencing with serum untargeted metabolomics, was employed to elucidate the underlying neuroprotective mechanisms. Results: ACCS treatment significantly reduced cerebral infarct volume, improved neurobehavioral function, and restored cerebral blood flow in the ischemic region. Furthermore, ACCS modulated gut microbial structure, restored microbial diversity and increased the abundance of beneficial bacterial populations. Meanwhile, ACCS ameliorated serum metabolic disturbances induced by MCAO. Conclusion: This study rationally designed a bioactive combination derived from a TCM formulae, establishing a polypharmacological strategy for the treatment of ischemic stroke.

Keywords: Shengmai San; active component combination; cerebral ischemia; gut microflora; non-targeted metabolomics

1. Introduction

Ischemic stroke (IS), characterized by high rates of disability and mortality, poses a serious threat to global health [1–3]. Pathologically, IS results from cerebral artery embolism or occlusion and involves complex mechanisms, including excitotoxicity, oxidative stress, mitochondrial dysfunction, and blood-brain barrier disruption [4]. Traditional Chinese medicine (TCM) formulae, recognized for multi-target, multi-pathway therapeutic properties, have demonstrated promising clinical efficacy in treating complex diseases such as IS [5–9]. However, the inherent polypharmacy of traditional formulae presents significant obstacles in identifying active components and elucidating the synergistic mechanisms. Therefore, the development of systematic strategies for the precise discovery of bioactive molecules from TCM formulae has emerged as a critical frontier in current research.

Shengmai San (SMS), a classical ternary herbal formula documented in the ancient Chinese medical text "*Yixue Qiyuan (Origins of Medicine)*" from the China's Jin Dynasty (12th century), is composed of *Panax ginseng* C. A. Mey. (Ren Shen), *Ophiopogon japonicus* (L. f.) Ker-Gawl. (Mai Dong), and *Schisandra chinensis* (Turcz.) Baill. (Wu Wei Zi) [10]. SMS is widely employed as an emergency medicine in TCM clinical practice [11–13]. Modern pharmacological studies have demonstrated the therapeutic effects of SMS on the cardiovascular, cerebrovascular, nervous, endocrine, and respiratory systems [14]. For instance, SMS has been shown to alleviate oxidative injury in permanent bilateral common carotid artery occlusion [15]. Moreover, intraperitoneal administration of SMS exerts neuroprotective effects against cerebral ischemia by modulating AMPK-mTOR-JNK signaling pathways and attenuating autophagosome formation [16]. Besides, SMS has demonstrated against Aβ-induced Alzheimer's disease and scopolamine-induced learning and memory decline [17,18]. Collectively, SMS exhibits diverse biological activities, imparting therapeutic benefits against multiple diseases.

Previous studies have identified several neuroprotective compounds in SMS, including ginsenosides (ginsenoside Rg1 and ginsenoside Rb1), steroidal saponins (ruscogenin and ophiopogonin D), and lignan derivatives (schisandrin A and schisandrin B) [19]. Individually, ginsenoside Rg1 improves neurological function in cerebral ischemia models [20,21]. Similarly, ruscogenin attenuates ischemic brain injury by suppressing inflammasome activation and reducing reactive oxygen species generation [22]. Furthermore, schisandrin A exerts neuroprotective effects through coordinated anti-inflammatory effects and autophagy induction [23]. These findings collectively underscore the neuroprotective potential of these compounds, highlighting promise for clinical translation.

Notably, recent advances suggest that systematically optimized multicomponent combinations derived from TCM formulae can achieve therapeutic efficacy by enhancing synergistic interactions while improving quality control [24–26]. In this study, we developed an active component combination (ACCS) comprising of ginsenoside Rg1, ruscogenin, and schisandrin A. We demonstrated that ACCS significantly reduced cerebral infarct volume, improved neurobehavioral performance, and restored regional cerebral blood flow in middle cerebral artery occlusion (MCAO) rats. Furthermore, ACCS treatment modulated gut microbiota composition, replenished microbial diversity, and ameliorated serum metabolic dysregulation. Taken together, our findings establish a methodology for identifying bioactive constituents in complex herbal formulations, thereby facilitating mechanistic exploration of therapeutic effects. These results further underscore the translational potential of ACCS as a naturally derived composite for ischemic stroke treatment.

2. Method

2.1. Materials

Panax ginseng C. A. Mey. (Ren Shen), *Ophiopogon japonicus* (L. f.) Ker-Gawl. (Mai Dong), *Schisandra chinensis* (Turcz.) Baill. (Wu Wei Zi) were purchased from Beijing Tong Ren Tang Technology Development (Beijing, China). Ginsenoside Rg1, ruscogenin, schisandrin A, and nimodipine (Nim) were purchased from Chengdu Desite Biotechnology (Chengdu, Sichuan, China). Round-tipped silicone-coated nylon sutures and isoflurane were purchased from RWD Life science (Shenzhen, Guangdong, China). The primary antibody and secondary antibody were purchased from Cell Signaling Technology (Beverly, MA, USA). Carboxymethyl cellulose sodium (CMC-Na) and bovine serum albumin (BSA) were purchased from Sigma (Poole, Dorset, UK). 4% paraformaldehyde solution was purchased from Solabio (Beijing, China). 3% H_2O_2, 5% goat serum, and DAB Substrate Kit were purchased from ZSGB-BIO (Beijing, China).

2.2. Preparation and Administration of SMS and ACCS

Preparation of SMS extract. The herbal mixture was subjected to extraction three times with five volumes of 70% ethanol under reflux for 1 h per cycle. After each extraction, the solution was filtered. The combined filtrates were concentrated to a thick paste using a rotary evaporator and subsequently lyophilized to yield the final powder. For administration, the SMS extract was dissolved in 5% CMC-Na and administered at a dose of 2 g/kg. Preparation of ACCS. These three compounds (Ginsenoside Rg1, ruscogenin, and schisandrin A) were combined in a weight ratio of 5: 3: 2 to form ACCS. The ACCS was dissolved in 5% CMC-Na and administered at a dose of 20 mg/kg. The positive control drug, Nim was dissolved in 5% CMC-Na and administered at a dose of 20 mg/kg.

2.3. Middle Cerebral Artery Occlusion (MCAO) Model

Male Sprague-Dawley (SD) rats, weighing 250–280 g, were obtained from the Animal Department of Peking University Health Science Center. Animals were housed under a 12 h light/dark cycle with free access to food and water. All animal experiments were approved by the Ethics Committee of Experimental Animal Ethics Committee of Peking University (DLASBE0819). Rats were randomly divided into five groups: sham group, MCAO group, MCAO + SMS group, MCAO + ACCS group, and MCAO + Nim group. The MCAO model was carried out as previously described [27]. Briefly, under isoflurane anesthesia, the common carotid artery (CCA), external carotid artery (ECA), and internal carotid artery (ICA) were exposed. The ECA was ligated and a round-tipped silicone-coated nylon suture was inserted into the ICA via CCA. The suture was gently advanced to occlude the right middle cerebral artery (MCA) at a depth of approximately 18–20 mm. After 1.5 h, the suture was withdrawn to allow reperfusion. Throughout the surgery, anesthesia was maintained with isoflurane, and body temperature was regulated at 37 °C using a heating pad. The sham and MCAO groups received 5% CMC-Na as vehicle control. The MCAO + SMS group, MCAO + ACCS group, and MCAO + Nim groups were respectively given the corresponding drugs. All treatments were administered once daily for 7 days.

2.4. Magnetic Resonance Imaging (MRI)

After the final drug administration, rats were anesthetized and placed in a supine position on the scanning bed. The head was secured within a dedicated experimental coil (40 mm), and scanning was performed using an MRI system (GE Healthcare, Waukesha, WI, USA). T2-weighted imaging was performed using a fast spin-echo sequence with the following parameters: repetition time (TR) = 3767 ms, echo time (TE) = 55.3 ms, field of view (FOV) = 4 cm, matrix size = 129 × 256, number of excitations (NEX) = 1, with 11 contiguous slices of 1.5 mm thickness. Image analysis was conducted using Image software. The coronal slice displaying the largest infarct area was selected for quantitative assessment of infarct volume.

2.5. Neurological Deficit Evaluation

Neurological deficits were evaluated using the Zea-Longa scoring system [28]. 0—normal, no neurological deficit; 1, mild neurological deficit, characterized by failure to fully extend the left forepaw; 2—moderate deficit, presenting with circling to the left; 3—severe deficit, exhibiting falling to the left; 4—no spontaneous movement with depressed consciousness; 5—death. Rats exhibiting scores between 1 and 3 were included in subsequent experimental procedures.

2.6. Laser Speckle Contrast Imaging (LSCI)

The animal was secured in a stereotaxic frame, and a cranial window (10 mm × 15 mm) was created. Cerebral blood flow (CBF) was monitored using a laser speckle contrast imaging system (RWD Life science) equipped with a 785 nm laser source and a complementary metal-oxide-semiconductor (CMOS) camera. The system was operated at a frame rate of 100 fps with a spatial resolution of 7.5 million/cm^2. The probe was positioned approximately 20 cm above the skull surface. The camera resolution was set at 2064 × 1544 pixels. Raw speckle images were processed by the system software to generate perfusion maps. The CBP in the infarct region was quantitatively assessed by comparing the mean signal intensity in the ischemic region with non-ischemic region.

2.7. Nissl Staining and Hematoxylin-Eosin (H&E) Staining

Brain tissues were collected and fixed with 4% paraformaldehyde for 24 h. The tissues were embedded in paraffin and sectioned into 5 μm thick slices. Sections underwent deparaffinization and rehydration, followed by Nissl staining and H&E staining, respectively. Stained sections were imaged using digital pathology slide scanner with digital pathology scanner (NanoZoomer, Hamamatsu Photonics, Hamamatsu, Japan).

2.8. Immunohistochemical (IHC) Staining

Brain tissue sections were prepared as described in Section 2.7. Subsequently, endogenous peroxidase activity was quenched by incubation with 3% H_2O_2. After blocking non-specific binding sites with 5% goat serum, the sections were then incubated overnight at 4 °C with MAP2 antibody. This was followed by a 1 h incubation at room temperature with an appropriate horseradish peroxidase (HRP)-conjugated secondary antibody. Antigen-antibody complexes were visualized using a DAB chromogen substrate kit. The imaged were captured with a digital slide scanner (NanoZoome) under bright-field illumination at 40× magnification.

2.9. 16S rRNA Gut Microbiota Analysis

The colon was exposed and well-formed fecal pellets were collected using sterile forceps into sterile tubes. Samples were stored at −80 °C until further processing. 16S rRNA V4 region sequencing was performed by Novogene (Beijing, China). Briefly, the V4 region was amplified using primers 5′-GTGCCAGCMGCCGCGGTAA-3′ and 5′-GGACTACHVGGGTWTCTAAT-3′ under the following PCR conditions: pre-denaturation at 98 °C for 1 min; 30 cycles of denaturation at 98 °C for 10 s, annealing at 50 °C for 30 s, and extension at 72 °C for 30 s and 72 °C for 5 min. Paired-end sequencing (PE250) was conducted on the Illumina NovaSeq 6000 platform. Raw sequences were processed using FLASH and fastp software for assembly and quality control. Sequences were clustered into operational taxonomic units (OTUs) at 97% sequence similarity. Subsequent analyses included alpha diversity, beta diversity, microbial community composition, and functional prediction.

2.10. Untargeted Metabolomics Analysis

Blood samples were collected in EDTA tubes. The supernatant was aliquoted and stored at −80 °C. Untargeted metabolomics analysis was conducted by Novogene. Chromatographic separation was performed using a Vanquish UHPLC system coupled with an Orbitrap Q Exactive™ HF mass spectrometer (Thermo Fisher,

Darmstadt, Germany). Mass spectrometric detection was conducted in both positive and negative polarity modes (scan range of 100–1500 Da) with specified parameters. Raw data were processed using Compound Discoverer 3.3 software for peak detection and alignment. Metabolites were identified by querying the mzCloud, mzVault, and Masslist databases and annotated using online databases including KEGG, HMDB, and LIPIDMAPS. Differential metabolites were selected with thresholds of variable importance in projection (VIP) > 1.0, fold change (FC) > 2 or FC < 0.5, with a statistical significance threshold of $p < 0.05$.

2.11. Statistical Analysis

Data were expressed as the mean ± SD. Statistical analysis was carried out using two-tailed Student's *t*-test for comparison between two groups and one-way analysis of variance (ANOVA), when the data involved three or more groups. $p < 0.05$ was defined as significant.

3. Results

3.1. ACCS Demonstrates Significant Neuroprotection against Cerebral Ischemia Injury in MCAO Rats

We formulated the active component combination (ACCS) by combining three representative components from SMS, ginsenoside Rg1, ruscogenin, and schisandrin A (Figure 1A), at a ratio of 5:3:2. This ratio was determined based on both the relative contents of these component in the source herbs and previous pharmacological evidence [14,19,29]. The ACCS, SMS, and Nim were treated in MCAO rats with oral administration to evaluate anti-cerebral ischemia efficacy (Figure 1B). Neurological deficits were evaluated using the Zea-Longa score. As shown in Figure 1C, MCAO led to significant neurological deficits, manifested as leaning, circling, and lateral tilting in severe cases. Both ACCS (20 mg/kg) and SMS (2 g/kg) treatments significantly ameliorated these neurological impairments compared to MCAO group. Subsequently, MRI revealed distinct hyperintense signals in the ischemic hemisphere, indicating cerebral infarction. In contrast, ACCS and SMS groups showed a marked reduction in infarct volume (Figure 1D). Furthermore, cerebral blood flow (CBF) was monitored in both the ischemic and non-ischemic regions through laser speckle contrast imaging (LSCI). As Shown in Figure 1E, MCAO caused a substantial decrease in CBF and a reduction in vascular density. ACCS and SMS effectively restored blood perfusion, increased vascular abundance, and mitigated the ischemic condition. Collectively, these findings demonstrated that ACCS exhibited a neuroprotective effect comparable to SMS extract against cerebral ischemia injury.

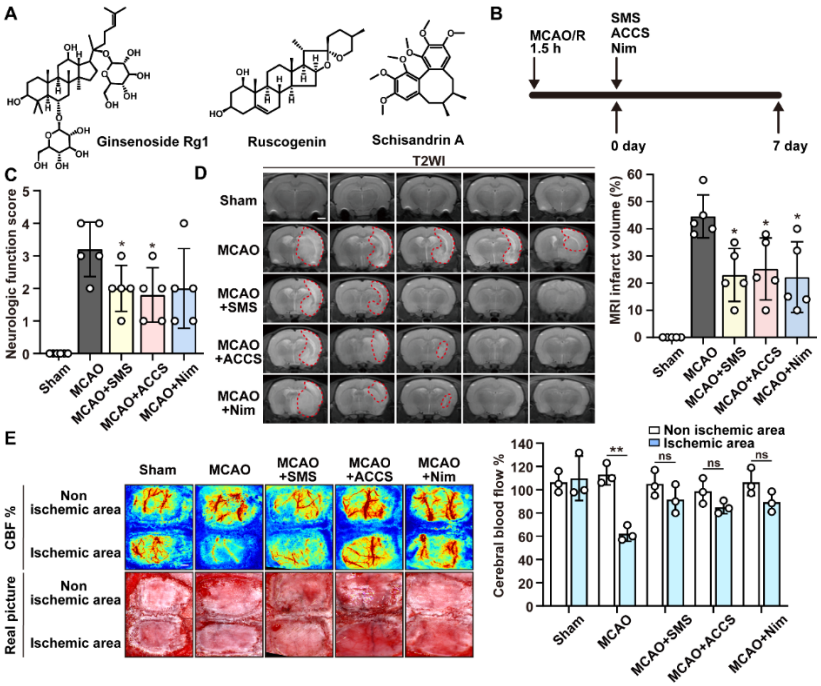

Figure 1. ACCS demonstrates significant neuroprotection against cerebral ischemia injury in MCAO rats. (**A**) The chemical structures of ginsenoside Rg1, ruscogenin, and schisandrin A. (**B**) Schematic diagram of the MCAO procedure and subsequent drug administration. (**C**) Assessment of neurological deficit scores using the Zea-Longa. (**D**) MRI detection of cerebral infarct area. Scale bar: 2000 μm. (**E**) LSCI was conducted to quantify CBF in ischemic and non-ischemic regions. Scale bar: 2000 μm. Data are expressed as mean ± SD. * $p < 0.05$, ** $p < 0.01$ compared to MCAO group; ns no significant.

3.2. ACCS Attenuates Neuronal Injury in MCAO Rats

To evaluate the neuroprotective potential of ACCS, we performed neuronal damage in the infarct region using Nissl and Hematoxylin-eosin (H&E) staining. In the sham group, neurons displayed a well-organized architecture, intact morphology, and abundant Nissl bodies (Figure 2A). In contrast, MCAO group exhibited severe histological disruption, including disorganized neuronal structure, pronounced edema and necrosis, and a marked reduction in Nissl bodies. ACCS and SMS ameliorated these pathological changes, restoring the brain tissue architecture and cellular morphology, although minor vacuolation persisted in some areas. Given that microtubule-associated protein 2 (MAP2) is a key cytoskeletal protein essential for maintaining neuronal morphology and process outgrowth [30]. We further performed immunohistochemical (IHC) analysis. The results revealed a significant decrease in MAP2-positive cells following MCAO, which was substantially reversed by both ACCS and SMS treatments (Figure 2B). Furthermore, H&E staining of major organs (heart, liver, spleen, lungs, and kidneys) showed no significant pathological changes following administration of either ACCS or SMS (Figure 2C). Therefore, these results demonstrated that ACCS effectively mitigates neuronal death in the infarct area without eliciting observable toxicity.

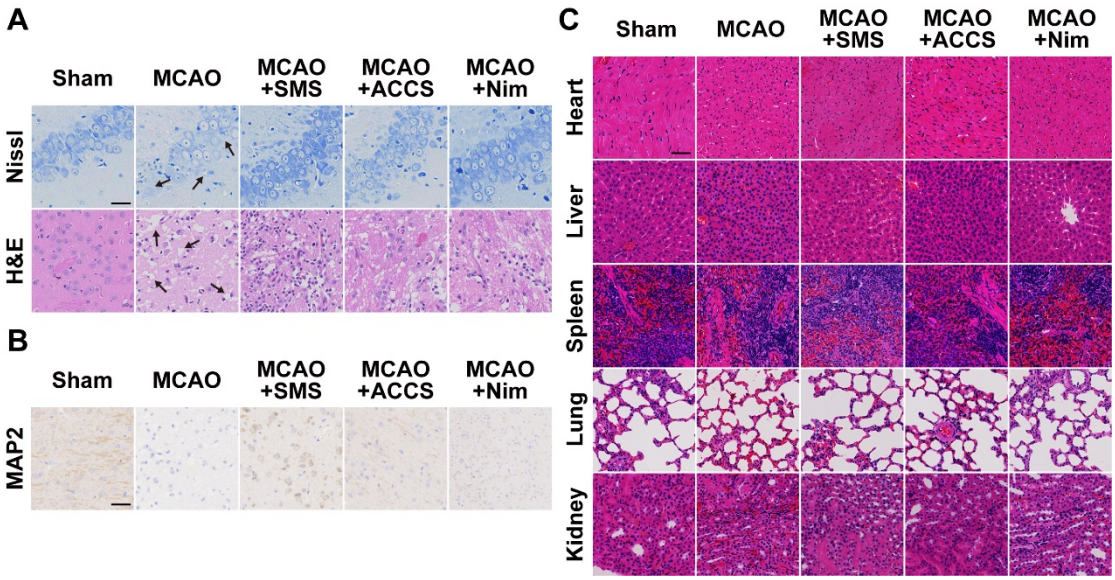

Figure 2. ACCS attenuates neuronal injury in MCAO rats. (**A**) Representative images of Nissl and H&E staining depicting neuronal morphology and integrity in brain tissue. Scale bar: 50 μm. (**B**) IHC analysis of MAP2 expression in the cerebral infarct area. Scale bar: 50 μm. (**C**) Histopathological assessment of major organs (heart, liver, spleen, lung, and kidney) by H&E staining. Scale bar: 50 μm.

3.3. ACCS Ameliorates Gut Microbial Dysbiosis in MCAO Rats

The homeostasis of gut microbiota plays a pivotal role in the progression of ischemic stroke [31]. To investigate the impact of ACCS on gut microbiota composition, colonic contents were collected and subjected to 16S rRNA sequencing. Principal coordinate analysis (PCoA) of beta diversity revealed a clear separation between the sham and MCAO groups, indicating substantial microbial dysbiosis after cerebral ischemia. Notably, ACCS and SMS shifted the microbial community structure toward a state resembling the sham group (Figure 3A). Alpha diversity analysis further demonstrated that MCAO significantly reduced the richness and diversity, as reflected by the Chao1 and Shannon indices, while the microbial homeostasis was reversed by ACCS treatments (Figure 3B,C).

We further explored microbial alterations at the genus levels (displaying the top 10 abundant genera) in Figure 3D. In sham group, *Ligilactobacillus*, *Prevotellaceae_UCG-003*, and *Prevotellaceae_NK3B31* were identified as the predominant genera. Compared with sham group, MCAO resulted in gut microbiota dysbiosis, characterized by an increased abundance of *Prevotella_9* and *Escherichia-Shigella*, along with a marked reduction in *Lactobacillus*, *Dubosiella*, *Prevotellaceae_UCG-003*, and *Prevotellaceae_NK3B31*. Treatment with ACCS or SMS might reverse MCAO-induced dysbiosis. Specifically, SMS counteracted the rise in *Escherichia-Shigella*, whereas ACCS enhanced the abundance of *Dubosiella* and *Prevotellaceae_NK3B31*. Additionally, *Lactobacillus*, a recognized probiotic genus with potential neuroprotective benefits in cerebral ischemia, was significantly increased by treatment with both ACCS and SMS [32]. *Dubosiella* and *Prevotellaceae_NK3B31*, two taxa are recognized as beneficial microbes, known to mitigate neuroinflammation and preserve intestinal barrier integrity

via production of short-chain fatty acids (SCFAs) [33]. Furthermore, functional prediction of the gut microbiota was performed using Tax4Fun. As shown in Figure 3E, MCAO suppressed microbial functions including lipid metabolism, metabolism of terpenoids and polyketides, and translation, which were subsequently restored by ACCS and SMS. Additionally, MCAO led to increased microbial functions related to cell motility and signal transduction, which were subsequently restored by ACCS and SMS. Thus, these findings indicate that ACCS and SMS effectively ameliorate gut microbiota dysbiosis and restore microbial metabolic function in MCAO rats.

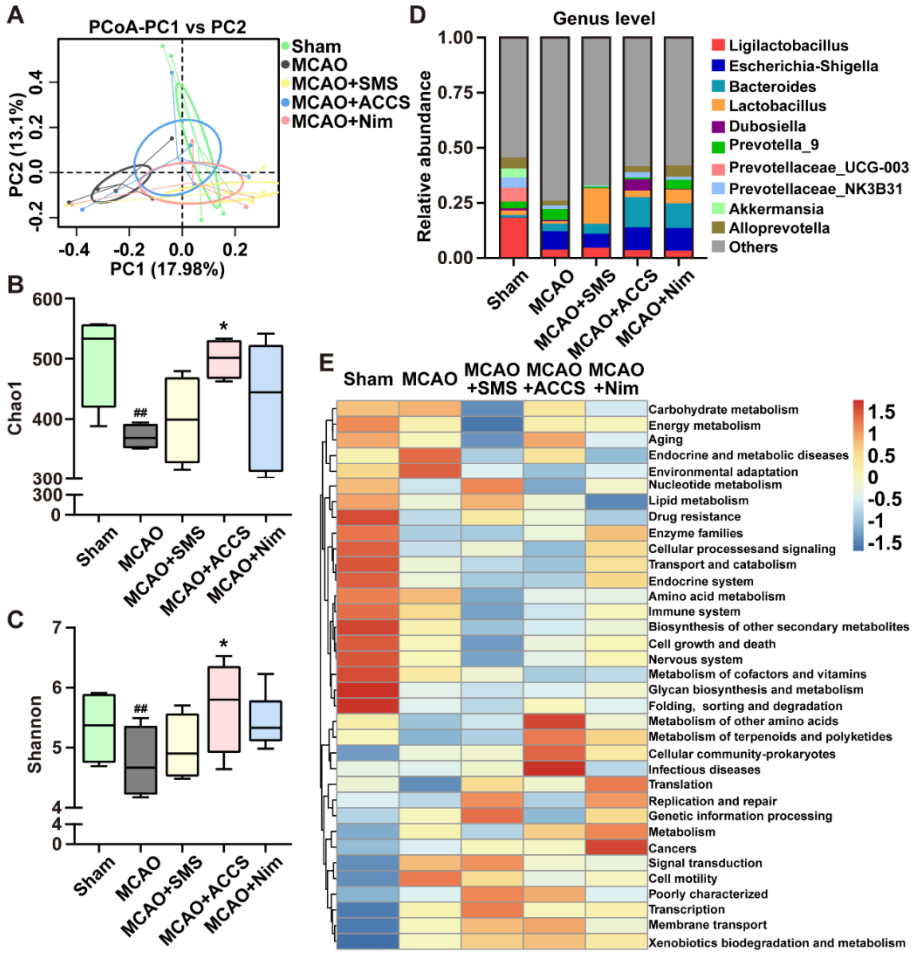

Figure 3. ACCS ameliorates gut microbial dysbiosis in MCAO rats. (**A**) PCoA showing the beta diversity of microbiome among different groups. (**B**,**C**) The alpha diversity of microbiome (Chao1 and Shannon index) among different groups. (**D**) Relative abundance at the genus level among different groups. (**E**) Functional prediction based on Tax4Fun. Data are expressed as mean ± SD. * $p < 0.05$, compared to MCAO group; $^{\#\#}$ $p < 0.01$ compared to sham group.

3.4. ACCS Alters Serum Metabolites in MCAO Rats

Given the established causal relationships between gut microbiota and metabolic dysfunction [34,35], we conducted untargeted metabolomics analysis of serum samples to investigate the systemic metabolic alterations. Principal component analysis (PCA) was performed to evaluate the distribution patterns among different groups under both positive and negative modes. The distinct clustering between the sham and MCAO groups reflected metabolic differences, while treatment with ACCS and SMS could partially reverse the metabolic abnormalities (Figure 4A,B).

A total of 852 and 452 metabolites were identified in the positive and negative modes, respectively. Hierarchical clustering analysis demonstrated distinct metabolite profiles across the experimental groups and MCAO group (Figure 4C,D). Differential metabolites were subsequently screened based on the criteria of VIP > 1.0, FC > 2 or < 0.5, and $p < 0.05$. In the positive mode, 201 differential metabolites were identified between the MCAO and sham groups, comprising 134 upregulated and 67 downregulated. Comparative analysis between the MCAO and ACCS groups revealed 68 differential metabolites, showing a predominant downregulation pattern (12 upregulated, 56 downregulated). Similarly, in the negative mode, 116 differential metabolites were detected between the MCAO and sham groups (53 upregulated, 63 downregulated), while 27 differential metabolites were identified between the MCAO and ACCS groups (10 upregulated, 17 downregulated) (not shown in paper). KEGG

pathway enrichment analysis of the differential metabolites between the MCAO and ACCS groups revealed significant enrichment in several key pathways, including vitamin digestion and absorption, pyrimidine metabolism, citrate cycle (TCA cycle), and tyrosine metabolism (Figure 4E,F). The modulation of these pathways suggests a multi-target mechanism underlying the systematic therapeutic potential of ACCS against cerebral ischemia.

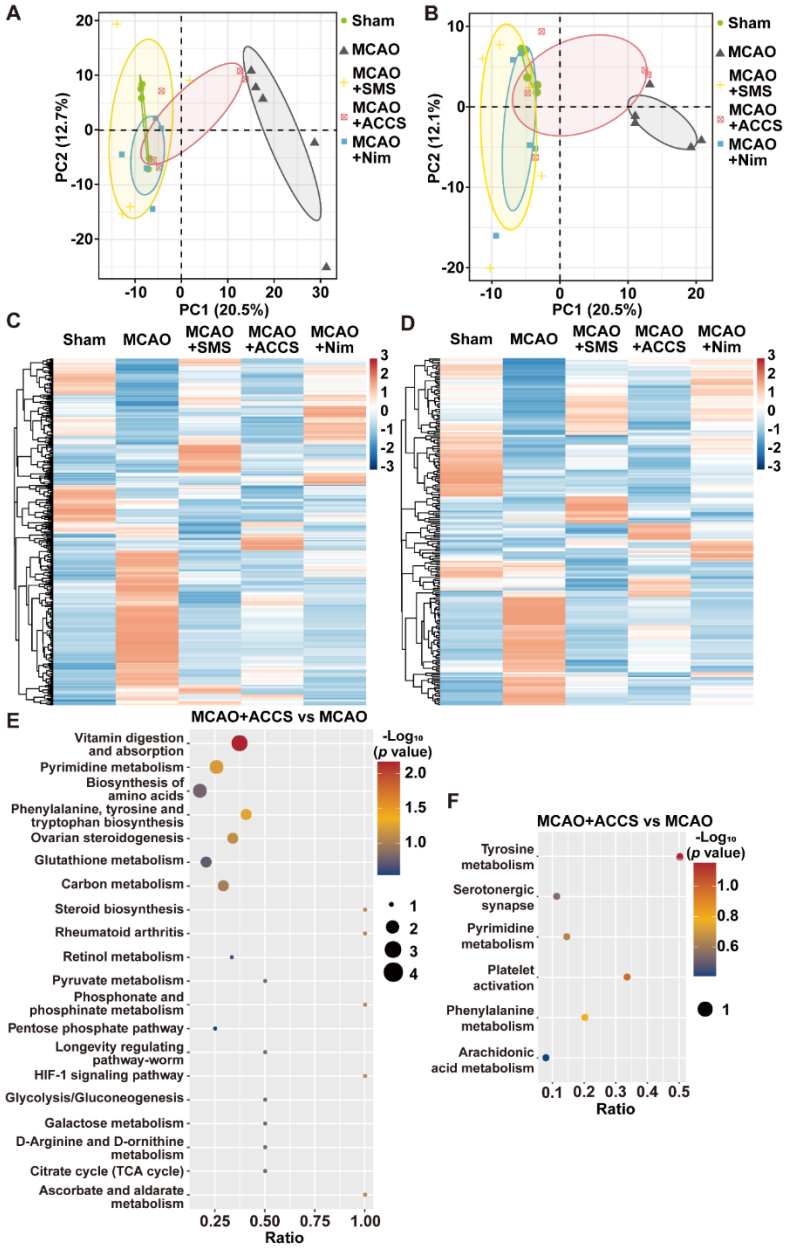

Figure 4. ACCS alters serum metabolites in MCAO rats. (**A**) Scores plots of PCA derived from serum metabolomic profiles in positive mode. (**B**) Scores plots of PCA derived from serum metabolomic profiles in negative mode. (**C**) Hierarchical clustering heatmap of differential metabolites identified in positive modes. (**D**) Hierarchical clustering heatmap of differential metabolites identified in negative modes. (**E**) KEGG pathway enrichment analysis of differential metabolites between the MCAO + ACCS and MCAO groups in positive modes. (**F**) KEGG pathway enrichment analysis of differential metabolites between the MCAO + ACCS and MCAO groups in negative modes.

3.5. ACCS Treatment Modulates Levels of Key Differential Metabolites

We further characterized specific alterations in metabolite levels. Specifically, the serum levels of multiple glycerophospholipid species, including LPC 18:0-SN2, LPE 16:0, LPC 16:0, LPC 12:0, and LysoPE 18:0 were markedly decreased in the MCAO group in both positive and negative mode (Figure 5A,B). These reductions were restored by ACCS and SMS treatment. Besides, in positive mode, we also observed a significant reduction in 3-hydroxyanthranilic acid during MCAO, a tryptophan metabolite implicated in inflammatory response during IS [36]. Conversely, the MCAO group exhibited elevated plasma levels of L-phenylalanine, nicotinamide, and

prostaglandin A3. ACCS and SMS normalized these elevations. SMS appeared to facilitates the conversion of L-phenylalanine into endogenous halogenated tyrosine analogs, such as 3,5-diiodo-L-tyrosine and 3,5-dibromo-L-tyrosine, which may contribute to neuroprotective effects [37]. Nicotinamide, an essential precursor of NAD^+, plays a critical role in cerebral energy metabolism and redox homeostasis [38]. The disruption of nicotinamide metabolism following MCAO was effectively restored by ACCS and SMS administration. Furthermore, the elevation of prostaglandin A3, implicated in exacerbating post-ischemic inflammatory damage, was notably attenuated by ACCS treatment [39]. In negative mode, MCAO induction significantly increased plasma concentrations of cholic acid, N1-[4-(aminosulfonyl)phenyl]-2,2-dimethylpropanamide, and indole-3-lactic acid. ACCS and SMS treatments partially or completely reduced all three metabolites (Figure 5A,B).

Ischemia-associated gut dysfunction perturbs enterohepatic circulation of bile acids, leading to cholic acid accumulation, which in turn promotes reactive oxygen species generation and inflammasome activation, aggravating neuroinflammation [40]. ACCS effectively attenuated cholic acid elevation. Indole-3-lactic acid, a gut microbial metabolite derived from *Bifidobacterium* and *Lactobacillus*, is often elevated under inflammatory conditions [41,42]. The reduction in indole-3-lactic acid levels following ACCS administration suggests the modulatory role in gut-brain axis signaling. To further explore the potential microbiota-gut-brain axis mechanisms, we performed a correlation analysis between significantly altered metabolites and gut microbiota at the genus level using Pearson's correlation coefficients. As shown in the Figure 5C, *Bacteroides* exhibited a significant positive correlation with LPC 12:0 and LPE 16:0, but a significant negative correlation with Prostaglandin A3. Meanwhile, 3-hydroxyanthranilic acid and LPC 18:0-SN2 showed significant negative correlations with *Prevotellaceae_NK3B31_group* and *Akkermansia*, respectively. Collectively, these findings demonstrate that ACCS, alongside SMS, can effectively reverse the systemic metabolic disturbances induced by cerebral ischemia.

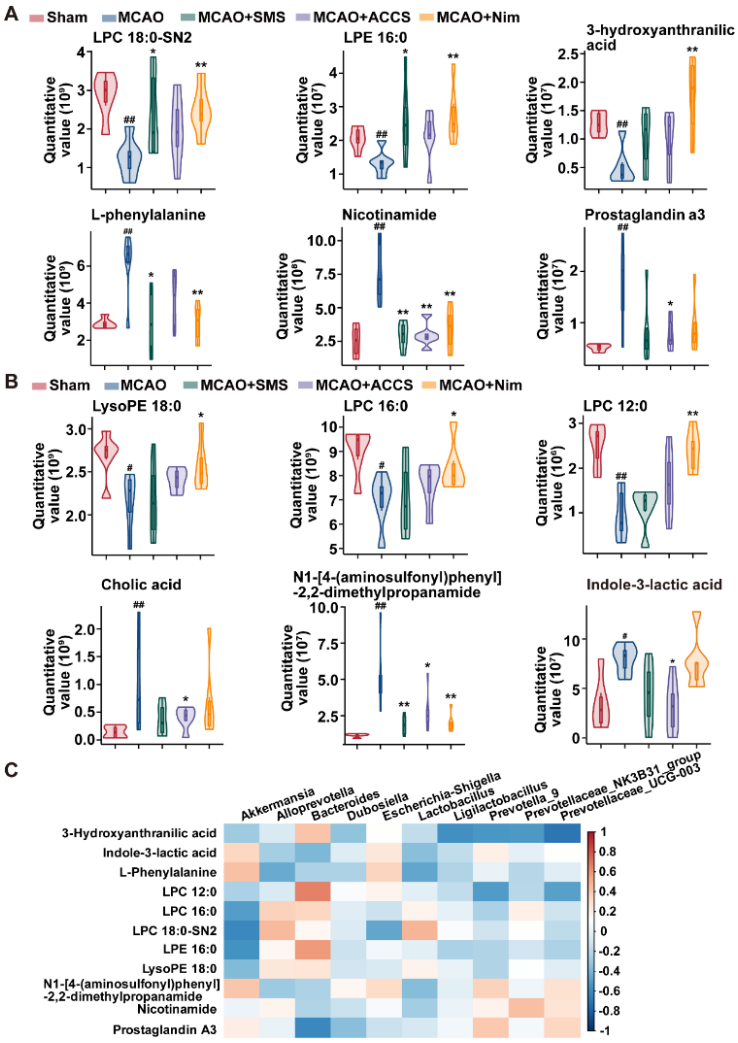

Figure 5. ACCS treatment modulates levels of key differential metabolites. (**A**) Differential metabolites in positive patterns among different groups. (**B**) Differential metabolites in negative patterns among different groups. (**C**) The correlation between the gut microbes and plasma metabolites. Data are expressed as mean ± SD. * $p < 0.05$, ** $p < 0.01$ compared to MCAO group; $^{\#}$ $p < 0.05$, $^{\#\#}$ $p < 0.01$ compared to sham group.

4. Discussion

Previous studies have shown that active constituents derived from TCM formulae exert unexpectedly potent therapeutic efficacy against ischemic stroke [43,44]. The use of TCM formulae is evolving from extracts to precisely defined multi-component combinations [45–47]. In our research, the ACCS combination (ginsenoside Rg1, ruscogenin, and schisandrin A) was rationally designed based on TCM compatibility principles to achieve synergistic neuroprotection. The 5:3:2 ratio of these components was optimized according to the natural abundance in the source herbs and established pharmacological evidence [19]. Our findings demonstrated that ACCS significantly alleviated cerebral ischemia injury, as evidenced by reduced infarct volume, restored cerebral blood flow, and improved neurobehavioral function. Thus, these findings indicated that ACCS exhibits neuroprotective efficacy comparable to the original SMS formulation. This strategy of optimizing component combinations provides a robust approach for the standardization and quality control of complex formulae. Thus, the ACCS combination presents a promising candidate for developing innovative therapeutics against ischemic stroke.

Of note, we observed that ACCS exhibited remarkable neuroprotective effects by maintaining neuronal morphology, particularly preventing ischemia-induced reduction of Nissl bodies. This morphological preservation suggested the stabilization of critical cellular ultrastructure and synaptic architecture, which may contribute to functional recovery by promoting the reorganization and restoration of damaged neural networks following ischemic injury. Meanwhile, our findings indicated that the preservation of MAP2-positive cell may play a critical role in neuronal survival and functional recovery following stroke. Collectively, ACCS retains the core therapeutic activity of the original formula while offering advantages such as well-defined composition, improved quality control, and the potential reduction of ineffective or harmful components. Although these findings are promising, further investigation is necessary to confirm the retention of full synergistic efficacy and to comprehensively evaluate long-term safety through systematic toxicological studies.

Current findings demonstrate that the microbiota-gut-brain axis (MGBA) is increasingly recognized as a critical mediator of ischemic stroke pathology, integrating neural, endocrine, and metabolic signaling to modulate neuroinflammation and cerebrovascular repair [48]. Post-stroke dysbiosis, a well-established phenomenon, is characterized by diminished microbial diversity and an altered microbial composition, thereby influencing the production of gut microbiota-derived metabolites such as short-chain fatty acids and trimethylamine N-oxide [49,50]. Therefore, our study identified the ACCS as a promising potential candidate capable of modulating brain function through the restoration of gut microbiota homeostasis. However, the current study has several limitations that warrant further investigation. Future research should focus on precisely identifying the microbial species and enzymatic pathways responsible for generating these bioactive metabolites following ACCS treatment, as well as elucidating the molecular targets and downstream signaling pathways of these metabolites within the brain.

5. Conclusions

ACCS, a natural bioactive combination of ginsenoside Rg1, ruscogenin, and schisandrin A, which exhibits significant neuroprotective effects against cerebral ischemia injury. Thus, ACCS holds translational promise for clinical ischemic stroke treatment.

Author Contributions: K.-W.Z.: conceived and supervised the project; L.L., Z.Y., and Z.-K.C.: writing original draft, formal analysis, data curation; T.-T.W., P.-F.T., Y.Z., and B.-W.P.: provided technical services. All authors have read and agreed to the published version of the manuscript.

Funding: This work was supported by Beijing Municipal Natural Science Foundation (7232273), Guizhou Provincial Workstation for Leading Science & Technology Innovation Talents in Traditional Chinese Medicine Chemical Biology (QianKeHe platform-KXJZ[2025]033), and Joint Research Project of the Shijiazhuang-Peking University Cooperation Program.

Institutional Review Board Statement: All animal experiments were conducted in accordance with the relevant ethical guidelines and regulations. The experiments were approved by the Ethics Committee of Experimental Animal Ethics Committee of Peking University (DLASBE0819).

Informed Consent Statement: Not applicable.

Data Availability Statement: The data that support the findings of this study are available from the corresponding author upon reasonable request.

Conflicts of Interest: The authors declare no conflict of interest.

Use of AI and AI-Assisted Technologies: No AI tools were utilized for this paper.

Abbreviations

TCM	traditional Chinese medicine
SMS	shengmai san
MCAO	middle cerebral artery occlusion
IS	ischemic stroke
ACCS	active component combination
CMC-Na	sodium carboxymethyl cellulose
Nim	nimodipine
BSA	bovine serum albumin
OTUs	operational taxonomic units
VIP	variable importance in projection
FC	fold change
MRI	magnetic resonance imaging
PCoA	principal coordinate analysis
PCA	principal component analysis
LSCI	laser speckle contrast imaging
CBF	cerebral blood flow
IHC	immunohistochemistry
H&E	hematoxylin-eosin
MGBA	microbiota-gut-brain axis

References

1. Feigin, V.L.; Brainin, M.; Norrving, B.; et al. World Stroke Organization: Global Stroke Fact Sheet 2025. *Int. J. Stroke* **2025**, *20*, 132–144.
2. Prust, M.L.; Forman, R.; Ovbiagele, B. Addressing Disparities in the Global Epidemiology of Stroke. *Nat. Rev. Neurol.* **2024**, *20*, 207–221.
3. Zhang, S.; Wang, D.; Li, L. Recombinant Tissue-Type Plasminogen Activator (rt-PA) Effectively Restores Neurological Function and Improves Prognosis in Acute Ischemic Stroke. *Am. J. Transl. Res.* **2023**, *15*, 3460–3467.
4. Qin, C.; Yang, S.; Chu, Y.H.; et al. Signaling Pathways Involved in Ischemic Stroke: Molecular Mechanisms and Therapeutic Interventions. *Signal Transduct. Target Ther.* **2022**, *7*, 215.
5. Wang, S.; Hu, Y.; Tan, W.; et al. Compatibility Art of Traditional Chinese Medicine: From the Perspective of Herb Pairs. *J. Ethnopharmacol.* **2012**, *143*, 412–423.
6. Chen, B.; Jin, W. A Comprehensive Review of Stroke-Related Signaling Pathways and Treatment in Western Medicine and Traditional Chinese Medicine. *Front. Neurosci.* **2023**, *17*, 1200061.
7. Fan, G.; Liu, M.; Liu, J.; et al. Traditional Chinese Medicines Treat Ischemic Stroke and Their Main Bioactive Constituents and Mechanisms. *Phytother. Res.* **2024**, *38*, 411–453.
8. Cao, G.S.; Ye, X.Y.; Xu, Y.Q.; et al. YiQiFuMai Powder Injection Ameliorates Blood-Brain Barrier Dysfunction and Brain Edema after Focal Cerebral Ischemia-Reperfusion Injury in Mice. *Drug Des. Devel. Ther.* **2016**, *10*, 315–325.
9. Zhang, J.H.; Zhu, Y.; Fan, X.; et al. Efficacy-Oriented Compatibility for Component-Based Chinese Medicine. *Acta Pharmacol. Sin.* **2015**, *36*, 654–658.
10. Dong, J.Q.; Ma, Q.; Yang, R.; et al. Sheng Mai San Mitigates Heat Stress-Induced Myocardial Injury by Coordinated Regulation of the Keap1-Nrf2-HO-1 and Stub1-HSF1 Signaling Pathways. *Antioxidants* **2025**, *14*, 1140.
11. Zhang, B.R.; Liu, X.H.; Ling, Y.T.; et al. Effectiveness and Safety of Shengmai San for Viral Myocarditis: A Systematic Review and Meta-Analysis of Randomized Controlled Trials. *Cardiovasc. Ther.* **2024**, *2024*, 2127018.
12. Zhang, X.N.; Li, Y.Y.; Zhang, Y.H.; et al. Shengmai San for Treatment of Cardiotoxicity from Anthracyclines: A Systematic Review and Meta-Analysis. *Chin. J. Integr. Med.* **2022**, *28*, 374–383.
13. Lee, M.M.L.; Chan, B.D.; Ng, Y.W.; et al. Therapeutic Effect of Sheng Mai San, a Traditional Chinese Medicine Formula, on Inflammatory Bowel Disease via Inhibition of NF-κB and NLRP3 Inflammasome Signaling. *Front. Pharmacol.* **2024**, *15*, 1426803.
14. Yi, O.Y.; Tang, L.Y.; Hu, S.W.; et al. Shengmai San-Derived Compound Prescriptions: A Review on Chemical Constituents, Pharmacokinetic Studies, Quality Control, and Pharmacological Properties. *Phytomedicine* **2022**, *107*, 154433.
15. Wang, X.J.; Magara, T.; Konishi, T. Prevention and Repair of Cerebral Ischemia-Reperfusion Injury by Chinese Herbal Medicine, Shengmai San, in Rats. *Free Radic. Res.* **1999**, *31*, 449–455.
16. Yang, H.P.; Li, L.; Zhou, K.C.; et al. Shengmai Injection Attenuates the Cerebral Ischemia/Reperfusion Induced Autophagy via Modulation of the AMPK, mTOR and JNK Pathways. *Pharm. Biol.* **2016**, *54*, 2288–2297.
17. Giridharan, V.V.; Thandavarayan, R.A.; Konishi, T. Effect of Shengmai-San on Cognitive Performance and Cerebral Oxidative Damage in BALB/c Mice. *J. Med. Food* **2011**, *14*, 601–609.

18. Lu, S.W.; Han, Y.; Chu, H.; et al. Characterizing Serum Metabolic Alterations of Alzheimer's Disease and Intervention of Shengmai-San by Ultra-Performance Liquid Chromatography/Electrospray Ionization Quadruple Time-of-Flight Mass Spectrometry. *Food Funct.* **2017**, *8*, 1660–1671.
19. Wang, Y.H.; Qiu, C.; Wang, D.W.; et al. Identification of Multiple Constituents in the Traditional Chinese Medicine Formula Sheng-Mai San and Rat Plasma after Oral Administration by HPLC-DAD-MS/MS. *J. Pharm. Biomed. Anal.* **2011**, *54*, 1110–1127.
20. Zhou, Y.; Li, H.Q.; Lu, L.; et al. Ginsenoside Rg1 Provides Neuroprotection against Blood Brain Barrier Disruption and Neurological Injury in a Rat Model of Cerebral Ischemia/Reperfusion through Downregulation of Aquaporin 4 Expression. *Phytomedicine* **2014**, *21*, 998–1003.
21. Yang, S.J.; Wang, J.J.; Cheng, P.; et al. Ginsenoside Rg1 in Neurological Diseases: From Bench to Bedside. *Acta Pharmacol. Sin.* **2023**, *44*, 913–930.
22. Cao, G.S.; Jiang, N.; Hu, Y.; et al. Ruscogenin Attenuates Cerebral Ischemia-Induced Blood-Brain Barrier Dysfunction by Suppressing TXNIP/NLRP3 Inflammasome Activation and the MAPK Pathway. *Int. J. Mol. Sci.* **2016**, *17*, 1418.
23. Zhi, Y.H.; Jin, Y.X.; Pan, L.L.; et al. Schisandrin A Ameliorates MPTP-Induced Parkinson's Disease in a Mouse Model via Regulation of Brain Autophagy. *Arch. Pharm. Res.* **2019**, *42*, 1012–1020.
24. Li, F.; Fan, X.X.; Chu, C.; et al. A Strategy for Optimizing the Combination of Active Components Based on Chinese Medicinal Formula Sheng-Mai-San for Myocardial Ischemia. *Cell. Physiol. Biochem.* **2018**, *45*, 1455–1471.
25. Zhu, L.; Liu, L.L.; Hou, L.H.; et al. Exploring the Effective Components and Mechanism of Shengmaiyin (Dangshen Prescription) on the Treatment of Chronic Heart Failure Based on Chinmedomics Strategy. *J. Pharm. Biomed. Anal.* **2025**, *243*, 117199.
26. Yang, W.W.; Lai, Q.; Zhang, L.; et al. Mechanisms Dissection of the Combination GRS Derived from ShengMai Preparations for the Treatment of Myocardial Ischemia/Reperfusion Injury. *J. Ethnopharmacol.* **2021**, *264*, 113381.
27. Liu, F.; McCullough, L.D. Middle Cerebral Artery Occlusion Model in Rodents: Methods and Potential Pitfalls. *Biomed. Res. Int.* **2011**, *2011*, 464701.
28. Longa, E.Z.; Weinstein, P.R.; Carlson, S.; et al. Reversible Middle Cerebral Artery Occlusion without Craniectomy in Rats. *Stroke* **1989**, *20*, 84–91.
29. Zhan, S.; Ding, B.; Ruan, Y.E.; et al. A Simple Blood Microdialysis in Freely-Moving Rats for Pharmacokinetic-Pharmacodynamic Modeling Study of Shengmai Injection with Simultaneous Determination of Drug Concentrations and Efficacy Levels in Dialysate. *J. Pharm. Biomed. Anal.* **2018**, *154*, 23–30.
30. Mages, B.; Fuhs, T.; Aleithe, S.; et al. The Cytoskeletal Elements MAP2 and NF-L Show Substantial Alterations in Different Stroke Models While Elevated Serum Levels Highlight Especially MAP2 as a Sensitive Biomarker in Stroke Patients. *Mol. Neurobiol.* **2021**, *58*, 4051–4069.
31. Hu, W.; Kong, X.; Wang, H.; et al. Ischemic Stroke and Intestinal Flora: An Insight into Brain-Gut Axis. *Eur. J. Med. Res.* **2022**, *27*, 73.
32. Ma, Y.; Liu, T.; Fu, J.; et al. *Lactobacillus acidophilus* Exerts Neuroprotective Effects in Mice with Traumatic Brain Injury. *J. Nutr.* **2019**, *149*, 1543–1552.
33. Li, W.; Fu, X.; Lin, D.; et al. Conjugated linoleic acid alleviates glycolipid metabolic disorders by modulating intestinal microbiota and short-chain fatty acids in obese rats. *Food Funct.* **2023**, *14*, 1685–1698.
34. Mao, P.T.; Hu, J.H.; Mai, X.; et al. Multi-Omics Analysis of the Gut-Brain Axis Elucidates Therapeutic Mechanisms of Guhong Injection in the Treatment of Ischemic Stroke. *Int. J. Mol. Sci.* **2025**, *26*, 1560.
35. Shi, Y.Y.; Du, Q.Z.; Li, Z.L.; et al. Multiomics Profiling of the Therapeutic Effect of Dan-deng-tong-nao Capsule on Cerebral Ischemia-Reperfusion Injury. *Phytomedicine* **2024**, *128*, 155335.
36. Darlington, L.G.; Forrest, C.M.; Mackay, G.M.; et al. On the Biological Importance of the 3-Hydroxyanthranilic Acid: Anthranilic Acid Ratio. *Int. J. Tryptophan Res.* **2010**, *3*, 51–59.
37. Kagiyama, T.; Glushakov, A.V.; Sumners, C.; et al. Neuroprotective Action of Halogenated Derivatives of L-Phenylalanine. *Stroke* **2004**, *35*, 1192–1196.
38. Li, H.R.; Liu, Q.; Zhu, C.L.; et al. β-Nicotinamide Mononucleotide Activates NAD+/SIRT1 Pathway and Attenuates Inflammatory and Oxidative Responses in the Hippocampus Regions of Septic Mice. *Redox Biol.* **2023**, *63*, 102745.
39. Umemura, K.; Tsukada, H.; Kakiuchi, T.; et al. PET Study of the Neuroprotective Effect of TRA-418, an Antiplatelet Agent, in a Monkey Model of Stroke. *J. Nucl. Med.* **2005**, *46*, 1931–1936.
40. Hua, Q.; Zhu, X.L.; Li, P.T.; et al. The Inhibitory Effects of Cholalic Acid and Hyodeoxycholalic Acid on the Expression of TNF alpha and IL-1β after Cerebral Ischemia in Rats. *Arch. Pharm. Res.* **2009**, *32*, 65–73.
41. Zhang, Q.Q.; Zhao, Q.; Li, T.; et al. *Lactobacillus plantarum*-Derived Indole-3-Lactic Acid Ameliorates Colorectal Tumorigenesis via Epigenetic Regulation of CD8+ T Cell Immunity. *Cell Metab.* **2023**, *35*, 943–960.
42. Li, Y.K.; Li, Q.X.; Yuan, R.S.; et al. *Bifidobacterium breve*-Derived Indole-3-Lactic Acid Ameliorates Colitis-Associated Tumorigenesis by Directing the Differentiation of Immature Colonic Macrophages. *Theranostics* **2024**, *14*, 2719–2735.

43. Zhang, A.H.; Sun, H.; Yuan, Y.; et al. An *in vivo* Analysis of the Therapeutic and Synergistic Properties of Chinese Medicinal Formula Yin-Chen-Hao-Tang Based on its Active Constituents. *Fitoterapia* **2011**, *82*, 1160–1168.
44. Zhang, Q.; Wang, J.S.; Zhang, C.; et al. The Components of Huang-Lian-Jie-Du-Decoction Act Synergistically to Exert Protective Effects in a Rat Ischemic Stroke Model. *Oncotarget* **2016**, *7*, 80872–80887.
45. Luan, X.; Zhang, L.J.; Li, X.Q.; et al. Compound-Based Chinese Medicine Formula: From Discovery to Compatibility Mechanism. *J. Ethnopharmacol.* **2020**, *254*, 112687.
46. Tang, Y.P.; Xu, D.Q.; Yue, S.J.; et al. Modern Research Thoughts and Methods on Bio-Active Components of TCM Formulae. *Chin. J. Nat. Med.* **2022**, *20*, 481–493.
47. Wang, Y.X.; Huang, Y.X.; Wang, X.H.; et al. Compatibility Mechanism of Chinese Medicine Formula: State of the Art and Perspectives. *Drug Comb. Ther.* **2023**, *5*, 6–14.
48. Peh, A.; O'Donnell, J.A.; Broughton, B.R.S.; et al. Gut Microbiota and Their Metabolites in Stroke: A Double-Edged Sword. *Stroke* **2022**, *53*, 1788–1801.
49. Yin, J.; Liao, S.X.; He, Y.; et al. Dysbiosis of Gut Microbiota with Reduced Trimethylamine-N-Oxide Level in Patients with Large-Artery Atherosclerotic Stroke or Transient Ischemic Attack. *J. Am. Heart Assoc.* **2015**, *4*, e002699.
50. Li, J.J.; Xu, Q.L.; Xu, X.M.; et al. Apigenin Protects Ischemic Stroke by Regulating Intestinal Microbiota Homeostasis, Regulates Brain Metabolic Profile. *Front. Pharmacol.* **2025**, *16*, 1553081.